Available online at www.sciencedirect.com
SCIENCE DIRECT®
Journal of Magnetic Resonance 167 (2004) 169–177
JMR Journal of Magnetic Resonance
www.elsevier.com/locate/jmr

Communication

Determination of the electron relaxation rates in paramagnetic metal complexes: applicability of available NMR methods

Malene Ringkjøbing Jensen and Jens J. Led*

Department of Chemistry, University of Copenhagen, The H.C. Ørsted Institute, Universitetsparken 5, DK-2100 Copenhagen Ø, Denmark

Received 10 October 2003; revised 3 December 2003

Abstract

Four different approaches for determining the electron relaxation rates in paramagnetic metallo-proteins are investigated, using a paramagnetic Ni^{2+} complex of a protein as an example. All four approaches rely on the determination of the longitudinal paramagnetic relaxation enhancements, R_{1p}, of the ^1H nuclei and the backbone ^{15}N nuclei. Three of the methods utilize the field dependence of the R_{1p} rates. It is found that the applicability of each of these methods depends on whether the fast-motion condition, $\omega_S^2\tau^2 \ll 1$, applies to the electron relaxation, ω_S being the Larmor frequency of the electron spin S and τ the correlation time of the electron relaxation. If the fast-motion condition is fulfilled, the electron relaxation rate can be obtained from the ratio of the R_{1p} rates of one or more protons at two magnetic field strengths (method A). On the other hand, if the fast-motion condition does not apply, more elaborate methods must be used that, in general, require a determination of the R_{1p} rates over a larger range of magnetic field strengths (method C). However, in the case of paramagnetic metal ions with relatively slow electron relaxation rates only two magnetic field strengths suffice, if the R_{1p} rates of a hetero nucleus are included in the analysis (method B). In the fourth method (method D), the electron relaxation is estimated as a parameter in a structure calculation, using distance constraints derived from proton R_{1p} rates at only one magnetic field strength. In general, only methods B and C give unambiguous electron relaxation rates.

Keywords: Paramagnetic metal ion; Electron relaxation rate; Nickel; Metal binding tag; Zero field splitting

1. Introduction

Paramagnetic metal ions are potential sources of information about the structure and function of metallo-proteins. The unpaired electrons of a paramagnetic metal ion located in a protein highly influence the chemical shift and the relaxation rates of the protein nuclei [1]. Indeed, nuclei located more than 20 Å from the metal can be affected by the paramagnetic ion, allowing structural information to be derived from the paramagnetic relaxation rates and the pseudo contact shifts. This in turn can be used to refine the solution structures of native metallo-proteins and nucleic acids [2–5]. Similar long-range structural information can be obtained by artificially incorporating a paramagnetic metal ion in a protein using metal binding tags [6–8]. Moreover, the paramagnetic relaxation and the pseudo contact shifts can give information about intermolecular interactions [9–11] and the biological function of metallo-proteins [12,13].

To obtain the protein structure information from the experimental paramagnetic relaxation enhancements, the relaxation rate of the unpaired electron(s) of the paramagnetic metal ion must be known. Here, we investigate four different NMR approaches for determining this relaxation rate. The metal ion used in the investigation is the paramagnetic Ni^{2+} ion, while the protein is *Escherichia coli* thioredoxin (Trx) extended at the N-terminus with a metal binding tag. The tag consists of two histidine residues and one proline residue (HHP). The metal ion binds to the imidazole rings of the two histidine residues, while the tag is attached to the protein by the proline residue. Previously, it was shown that this tag forms a well-defined complex with the Ni^{2+} ion, where each Ni^{2+} ion binds two protein molecules forming an asymmetric dimer [8].

* Corresponding author. Fax: +45-35350609.
E-mail address: led@kiku.dk (J.J. Led).

1090-7807/$ - see front matter © 2003 Elsevier Inc. All rights reserved.
doi:10.1016/j.jmr.2003.12.009

2. Theory

In all four approaches investigated here, the longitudinal relaxation of the nuclei of the metallo-protein is used as the source of information about the electron relaxation. Unlike the transverse nuclear relaxation the longitudinal relaxation is in most cases unaffected by the internal mobility and the exchange processes in the proteins [14], making the interpretation of the experimental relaxation data more straightforward.

The longitudinal relaxation rate, R_1, of the ligand nuclei in a complex containing a paramagnetic metal ion is given by:

$$R_1 = R_{1d} + R_{1p}. \tag{1}$$

Here, R_{1d} is the relaxation rate in an analogue diamagnetic compound and R_{1p} is the paramagnetic relaxation enhancement. The paramagnetic relaxation enhancement may contain contributions from the Fermi contact relaxation [15–17], the Curie spin relaxation [18,19], and the dipolar relaxation [20]. The Fermi contact relaxation is caused by the modulation of the electron–nucleus scalar coupling and is, therefore, important only for nuclei relatively close to the paramagnetic ion. The Curie spin relaxation arises from the dipolar interaction of the nuclear spin with the static magnetic moment of the electron spin. The Curie spin relaxation is modulated only by the rotational correlation time of the protein [18,19] and can, therefore, easily be taken into account if necessary. However, for small proteins like thioredoxin, the longitudinal relaxation is unaffected by this relaxation mechanism [1]. In such cases, only the relaxation arising from the dipolar interaction between the electron spin and the nuclear spin contributes to the longitudinal paramagnetic relaxation enhancement of the protein nuclei.

If the point dipole approximation applies, i.e., the unpaired electrons are located at the metal ion, the longitudinal paramagnetic relaxation enhancement is given by [20]:

$$R_{1p} = \frac{2}{15}\left(\frac{\mu_0}{4\pi}\right)^2 S(S+1) g_e^2 \mu_B^2 \gamma_I^2 r^{-6} \left[\frac{3\tau_{c,1}}{1+\omega_I^2\tau_{c,1}^2} + \frac{7\tau_{c,2}}{1+\omega_S^2\tau_{c,2}^2}\right]. \tag{2}$$

Eq. (2) also assumes that the g-tensor is isotropic, and that the zero field splitting (only for $S \geqslant 1$) is small compared to the electron Zeeman energy [1]. In Eq. (2), ω_I and ω_S are the Larmor frequencies of the nuclear spin I and the electron spin S, respectively. Furthermore, γ_I is the gyromagnetic ratio of the nuclear spin I, g_e is the electron g-factor, S is the electron spin quantum number, μ_B is the Bohr magneton, and μ_0 is the permeability of free space. Finally, r is the distance between the metal ion and the nucleus. In the absence of chemical exchange, the correlation times, $\tau_{c,1}$ and $\tau_{c,2}$, can be written as

$$\tau_{c,1} = (\tau_r^{-1} + R_{1e})^{-1}, \tag{3}$$

$$\tau_{c,2} = (\tau_r^{-1} + R_{2e})^{-1}. \tag{4}$$

Here, R_{1e} and R_{2e} are the longitudinal and the transverse electron relaxation rates, respectively, while τ_r is the correlation time for the rotational reorientation of the complex. In Eq. (2), the term involving the electron Larmor frequency, ω_S, is negligible, if $\omega_S^2\tau_{c,2}^2 \gg 1$. Since the electron Larmor frequency is $2 \times 10^{12}\ s^{-1}$ at a magnetic field strength of 11.74 T, this condition holds for most paramagnetic metal ions. Therefore, the term involving ω_S in Eq. (2) is important only for very fast transverse electron relaxation rates ($R_{2e} \approx 10^{12}\ s^{-1}$).

If the relaxation of the unpaired electrons of the paramagnetic metal ion is governed by a modulation of the zero field splitting in solution (only for $S \geqslant 1$), the longitudinal and the transverse electron relaxation rates take the form [21,22]:

$$R_{1e} = \frac{2\Delta^2}{50}(4S(S+1)-3)\left[\frac{\tau_v}{1+\omega_S^2\tau_v^2} + \frac{4\tau_v}{1+4\omega_S^2\tau_v^2}\right], \tag{5}$$

$$R_{2e} = \frac{\Delta^2}{50}(4S(S+1)-3)\left[3\tau_v + \frac{5\tau_v}{1+\omega_S^2\tau_v^2} + \frac{2\tau_v}{1+4\omega_S^2\tau_v^2}\right]. \tag{6}$$

Here, Δ^2 is the mean squared fluctuation of the zero field splitting and τ_v is the correlation time for the modulation of the zero field splitting. For the paramagnetic Ni^{2+} ion, the zero field splitting is the dominant electron relaxation mechanism [1].

If the chemical exchange between the metal-free (diamagnetic) and the metal-bound (paramagnetic) form of the protein is fast, the observed nuclear relaxation, R_{1o}, is given by [23]:

$$R_{1o} = R_{1d} + f_p R_{1p}. \tag{7}$$

Here, f_p is the fraction of the metal-bound protein molecules. Thus, the paramagnetic relaxation enhancement, R_{1p}, can be obtained from the variation of the observed longitudinal relaxation rates with the concentration of the paramagnetic metal ion. The paramagnetic relaxation enhancement can also be calculated using Eq. (1), that is, as the difference between the relaxation in the paramagnetic complex and the relaxation in an analogue diamagnetic complex.

3. Experimental

Uniformly ^{15}N-labeled HHP-tagged thioredoxin was prepared and purified as described previously [8].

The protein was dissolved in 90% H_2O/10% D_2O with 50 mM sodium chloride. The protein concentration was 1.0 mM in all NMR samples and 5 μL of 50 mM H_2O_2 was added to each sample (500 μL) to obtain the pure oxidized form of HHP-Trx. The pH was adjusted to 7.0 (meter reading) and the samples were sealed off under nitrogen. Coordination of the Ni^{2+} and the Zn^{2+} ions used as the paramagnetic probe and the diamagnetic reference, respectively, was achieved by addition of the appropriate amounts of $NiCl_2 \cdot 6H_2O$ and $ZnCl_2$ to the protein samples. The concentration of the paramagnetic Ni^{2+} ion was varied in the range from 0.0 to 1.0 mM, while the concentration of the diamagnetic Zn^{2+} ion was either 0.35 or 1.0 mM.

All NMR experiments were carried out at 298 K and at magnetic field strengths of 9.39, 11.74, 14.09, and 18.79 T using Varian Mercury 400 and Varian Unity Inova 500, 600, and 800 spectrometers. In all experiments, the ^1H carrier was placed on the HDO residual resonance located at 4.774 ppm at 298 K [24]. The longitudinal ^1H relaxation rates of the amide protons in the HHP-tagged thioredoxin were obtained from a series of two-dimensional partially relaxed spectra acquired using the inversion recovery (IR) ^1H–^{15}N HSQC pulse sequence. The applied relaxation delays were in the range from 0.01 to 8 s. The partly relaxed spectra were recorded in a random order and a recurrent manner to eliminate systematic errors [25]. The spectra were collected with t_2 data points between 1680 and 2560, and the number of t_1 slices was between 120 and 180. The sweep widths were between 7.0 and 12.5 kHz in the ^1H dimension and between 1.8 and 3.2 kHz in the ^{15}N dimension. The longitudinal relaxation rates were extracted from the spectra by an exponential three-parameter fit using peak intensity versus the delay times.

The ^{15}N longitudinal relaxation rates were measured at 11.74 T using the gradient sensitivity-enhanced pulse sequences [26]. The R_1 experiment was collected with 2048 t_2 data points, 160 t_1 slices, and 12 relaxation delays in the range from 0.010 to 1.911 s. The sweep widths were 10 and 2 kHz in the ^1H and ^{15}N dimensions, respectively. The ^{15}N R_1 relaxation rates were extracted from the spectra by an exponential two-parameter fit of the signal intensities versus the delay times.

4. Results and discussion

Four different methods (methods A–D) for determining the electron relaxation rates of paramagnetic metal ions were investigated, using the Ni^{2+} complex of HHP-tagged thioredoxin as the model compound.

4.1. Method A: determination of R_{1e} from the ratio of proton R_{1p} rates at two magnetic field strengths

The simplest method for determining the longitudinal electron relaxation rate, R_{1e}, uses the nuclear paramagnetic relaxation enhancements, R_{1p}, at two different magnetic field strengths [6,27]. This method is applicable when the electron relaxation rate is in the fast-motion regime, that is $\omega_S^2\tau^2 \ll 1$, τ being the correlation time of the electron relaxation. In that case, the following conditions apply according to Eqs. (5) and (6):

1. The electron relaxation rates are field independent.
2. The longitudinal and the transverse electron relaxation rates are identical.

The conditions 1 and 2 ensure that $\tau_{c,1}$ and $\tau_{c,2}$ are field independent and that $\tau_{c,1} = \tau_{c,2}$ (see Eqs. (3) and (4)). Therefore, the ratio of the R_{1p} rates of a given nucleus at two magnetic field strengths depends on only one unknown parameter, $\tau_{c,1}$, according to Eq. (2). However, the determination of the electron relaxation rate might still be ambiguous. This is illustrated in Fig. 1, which shows the variation of the ratio $R_{1p}^{11.74\,T}/R_{1p}^{18.79\,T}$ with the correlation time $\tau_{c,1}$ under these conditions. Thus, a field dependence corresponding to a ratio smaller than approximately 1.3 results in three possible values of the correlation time $\tau_{c,1}$. This ambiguity stems from the fact that the two terms within the brackets in Eq. (2) dominate at different correlation times, i.e., the solutions around $\tau_{c,1} \approx 10^{-12}$ s arise from the ω_S-dependent term, while the solutions above $\tau_{c,1} \approx 10^{-10}$ s arise from the ω_I-dependent term.

To investigate the applicability of method A to the Ni^{2+} complex of HHP-Trx, the R_{1p} rates of the amide protons in HHP-Trx were determined at 11.74 and 18.79 T. The R_{1p} rates were calculated using Eq. (7). The R_{1d} rates were obtained from a 1.0 mM sample of HHP-Trx containing 0.35 mM Zn^{2+}, while the R_{1o} rates were

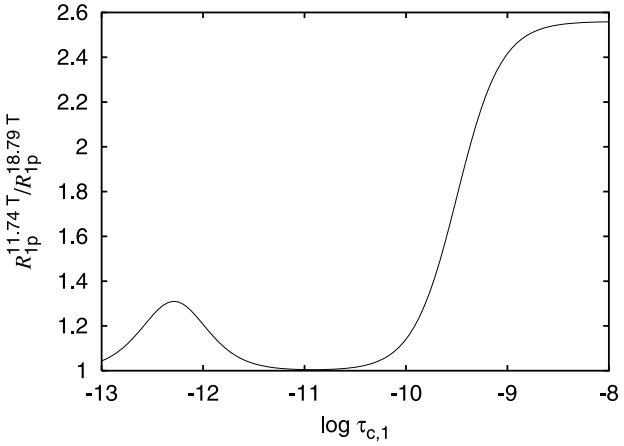

Fig. 1. The ratio of the paramagnetic relaxation enhancements at two different magnetic field strengths (11.74 and 18.79 T) calculated from Eq. (2). It is assumed that the electron relaxation rates are field independent and that $R_{1e} = R_{2e}$.

obtained from a 1.0 mM sample of HHP-Trx containing 0.35 mM Ni^{2+}. Since each Ni^{2+} ion binds two protein molecules [8], this corresponds to a fraction of Ni^{2+}-bound HHP-Trx, f_p, of 0.7.

The experimental data show that the ratios of the R_{1p} rates at 11.74 and 18.79 T of the individual amide protons in HHP-Trx are approximately constant throughout the entire protein sequence with a weighted average of 1.23 ± 0.02. According to Fig. 1 this ratio corresponds to three possible values of the correlation time $\tau_{c,1}$ and, thus, three values of the longitudinal electron relaxation rate, R_{1e}. Using Eq. (3) and the rotational correlation time $\tau_r = 8.76$ ns obtained previously for the Zn^{2+} complex of HHP-Trx [8], the following values of the longitudinal electron relaxation rates were obtained:

$$R_{1e} = \begin{cases} (7.0 \pm 0.3) \times 10^9\,s^{-1}, \\ (2.8 \pm 0.3) \times 10^{12}\,s^{-1}, \\ (1.4 \pm 0.2) \times 10^{12}\,s^{-1}. \end{cases} \quad (8)$$

Usually, the electron relaxation rate of the Ni^{2+} ion is in the range from 10^{10} to $10^{12}\,s^{-1}$ [1]. Therefore, none of the three solutions in Eq. (8) can be ruled out in the case investigated here.

For metal ions with slower electron relaxation rates, such as the Mn^{2+} and Cu^{2+} ions, the ω_S-dependent term in Eq. (2) is negligible, and only the solution corresponding to the $\tau_{c,1}$ value above approximately 10^{-10} s (Fig. 1) applies. In such cases unambiguous and reliable R_{1e} rates can be obtained from the field dependence of the nuclear R_{1p} rates [6]. Only if the field dependence of R_{1p} corresponds to $\tau_{c,1}$ values larger than approximately $10^{-9}\,s^{-1}$, the R_{1p} ratio becomes increasingly unaffected by variations in $\tau_{c,1}$, as shown in Fig. 1.

Finally, it should be noted that even if $\omega_S^2\tau^2 \ll 1$, the field dependence of R_{1p} is independent of the correlation time, $\tau_{c,1}$, if either $\omega_S^2\tau_{c,2}^2 \ll 1$ or $\omega_I^2\tau_{c,1}^2 \gg 1$. In the first limit, the ratio of the paramagnetic relaxation enhancements is equal to 1 according to Eq. (2), while in the second limit it is given by the square of the magnetic field ratio. Only a lower or an upper bound of the correlation time, $\tau_{c,1}$, can be obtained in these limits.

Unfortunately, it is normally unknown whether $\omega_S^2\tau^2 \ll 1$ and, thereby, whether the electron relaxation rates are field independent. Therefore, in general, other methods that are described below must be used.

4.2. Method B: determination of R_{1e} from the ratio of the R_{1p} rates of protons and hetero nuclei at two magnetic field strengths

If the condition $\omega_S^2\tau^2 \ll 1$ does not apply, the electron relaxation rates are field dependent and will, by themselves, give rise to a field dependence of R_{1p}, in addition to the field dependence of the Larmor frequency terms in Eq. (2). Therefore, R_{1p} rates at more than two magnetic field strengths must, in general, be used to determine all the involved parameters. However, if the ω_S-dependent term in Eq. (2) is negligible, the necessary field dispersion can be achieved with only two magnetic field strengths, by combining the R_{1p} rates of nuclei with different gyromagnetic ratios. Thus, it was shown previously [28] that a combination of R_{1p} rates of ^1H and ^{13}C nuclei at 11.74 and 17.61 T allows a determination of the R_{1e} rate of the Cu^{2+} ion in plastocyanin, as well as a determination of the field dependence of this rate. Since the ω_S-dependent term in Eq. (2) is negligible for this copper protein at the applied magnetic field strengths, R_{1p} will depend on only one correlation time, $\tau_{c,1}$, according to Eq. (2). Thus, for each kind of nucleus, i.e., ^1H and ^{13}C, the ratio $R_{1p}^{11.74\,T}/R_{1p}^{17.61\,T}$ depends on two unknowns, $\tau_{c,1}^{11.74\,T}$ and $\tau_{c,1}^{17.61\,T}$. However, the ratios for the ^1H and ^{13}C nuclei are different because of the different Larmor frequencies. Therefore, two equations in the two unknowns, $\tau_{c,1}^{11.74\,T}$ and $\tau_{c,1}^{17.61\,T}$, were obtained from the experimental $R_{1p}^{11.74\,T}/R_{1p}^{17.61\,T}$ ratios of the two kinds of nuclei, allowing the correlation times at the two field strengths to be determined.

Here, this approach was considered for the determination of the R_{1e} rate of the Ni^{2+} ion in HHP-Trx, using the $R_{1p}^{11.74\,T}/R_{1p}^{18.79\,T}$ ratios of the ^1H and ^{15}N nuclei in the protein. However, the approach is not applicable to this particular case for three reasons. First, the ω_S-dependent term in Eq. (2) may not be neglected for the Ni^{2+} complex of HHP-Trx because of a possible fast electron relaxation rate of the Ni^{2+} ion ($R_{1e} \approx 10^{12}\,s^{-1}$, see Eq. (8)). Second, $R_{1e} \neq R_{2e}$ since the electron relaxation is not in the fast-motion regime ($\omega_S^2\tau_v^2 \ll 1$ does not apply). Consequently, four unknowns, $\tau_{c,1}^{11.74\,T}$, $\tau_{c,1}^{18.79\,T}$, $\tau_{c,2}^{11.74\,T}$, and $\tau_{c,2}^{18.79\,T}$, are involved. Third, the R_{1p} rates of the ^{15}N nuclei are considerably smaller than those of the ^{13}C and ^1H nuclei for the same distance from the Ni^{2+} ion, because of the smaller ^{15}N gyromagnetic ratio. This is illustrated in Fig. 2 for a metal nucleus distance of 10 Å. Thus, the R_{1p} rate of the ^{15}N nuclei at this distance nearly vanishes for correlation times shorter than $10^{-10}\,s^{-1}$, while the R_{1p} rate of ^{13}C is still measurable, and the R_{1p} rate of ^1H is significant.

In accordance with this, the experimental ^{15}N R_1 relaxation rates (data not shown) in a sample containing an equivalent amount of Ni^{2+} are comparable to the R_1 relaxation rates of the ^{15}N nuclei in a sample with an equivalent amount of Zn^{2+}. Therefore, the backbone nitrogens of HHP-Trx are located too far from the Ni^{2+} ion to be affected by the unpaired electrons. In fact, slightly negative R_{1p} rates were obtained for some of the ^{15}N nuclei, indicating a difference between the rotational correlation times of the Ni^{2+} and the Zn^{2+} HHP-Trx dimer complexes.

Thus, method B might be the method of choice in cases of metal ions with relatively slow electron relaxation rates, such as Cu^{2+} and Mn^{2+}, where the ω_S-dependent term in Eq. (2) can be neglected. This holds in

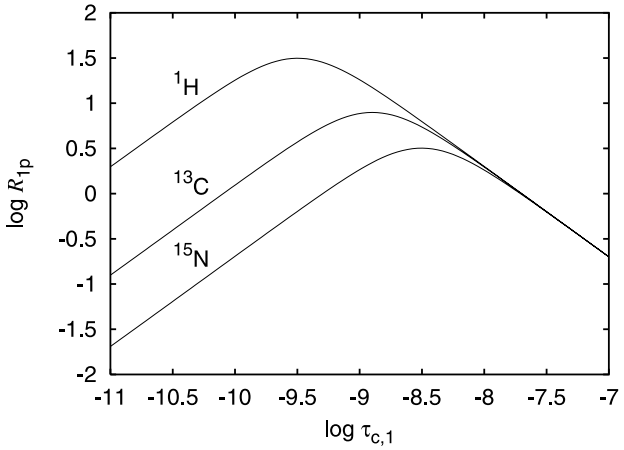

Fig. 2. The paramagnetic relaxation enhancement, R_{1p}, for ^{1}H, ^{13}C, and ^{15}N nuclei as a function of the correlation time, $\tau_{c,1}$. The curves were calculated using Eq. (2) and $S = 1$, $B_0 = 11.74$ T, and $r = 10$ Å. It was assumed that $R_{1e} = R_{2e}$.

particular if ^{13}C is used as the hetero nucleus. However, in the case of metal ions with relatively fast electron relaxation rates, where the ω_S-dependent term in Eq. (2) cannot be neglected, the methods discussed below are more applicable.

4.3. Method C: determination of R_{1e} and R_{2e} from proton R_{1p} rates over a wide range of magnetic field strengths

If neither the condition $\omega_S^2\tau^2 \ll 1$ applies nor can the ω_S-dependent term in Eq. (2) be neglected, a more rigorous method for determining the electron relaxation rates must be applied, where all the unknown parameters that affect the electron relaxation are determined. This, in turn, requires that the mechanism for the electron relaxation is known. In the case of paramagnetic Ni^{2+} complexes in solution, the dominant mechanism for the electron relaxation is a modulation of the zero field splitting [29]. Therefore, the R_{1e} and R_{2e} rates of the Ni^{2+} ion are given by Eqs. (5) and (6), where the unknown parameters are τ_v and Δ.

In most paramagnetic Ni^{2+} complexes, the electron relaxation rates, R_{1e} and R_{2e}, dominate the correlation times, $\tau_{c,1}$ and $\tau_{c,2}$, for the nuclear relaxation, R_{1p}. Thus, using Eqs. (2)–(6), the electron relaxation parameters, τ_v and Δ, can in principle be determined from the field dependence of the R_{1p} rates, together with the corresponding metal–nucleus distance, r.

To investigate the dependence of the nuclear relaxation on τ_v and Δ, the field dependence of the proton R_{1p} rates was plotted for different values of the two parameters, as shown in Fig. 3. The R_{1e} and R_{2e} rates were calculated using Eqs. (5) and (6) and values of τ_v and Δ normally observed in paramagnetic Ni^{2+} complexes [30]. The metal–nucleus distance was $r = 15$ Å and the electron spin was $S = 1$. As illustrated in Figs. 3A and B, the field dependence of R_{1p} varies considerably with the

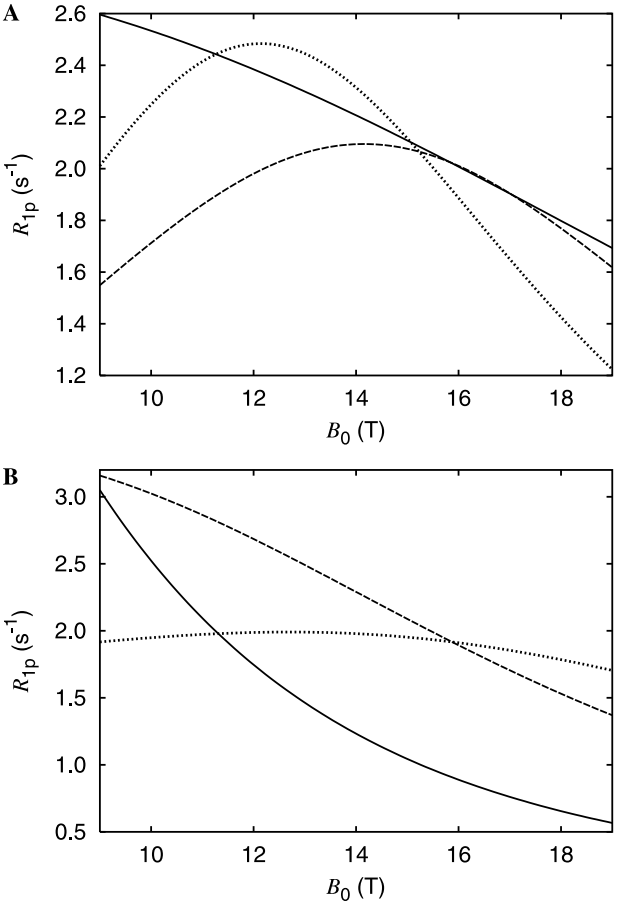

Fig. 3. The field dependence of the proton R_{1p} rates for different values of τ_v and Δ, assuming that the mechanism of the electron relaxation is a modulation of the zero field splitting. The R_{1e} and R_{2e} rates were calculated using Eqs. (5) and (6), the metal–nucleus distance $r = 15$ Å, and the electron spin $S = 1$. The R_{1p} curves were calculated using Eqs. (2)–(4). (A) The field dependence of R_{1p} for three different values of the correlation time, τ_v, assuming a constant zero field splitting $\Delta = 1.3\,cm^{-1}$; continuous curve, $\tau_v = 1 \times 10^{-13}$ s; dashed curve, $\tau_v = 5 \times 10^{-13}$ s; dotted curve, $\tau_v = 1 \times 10^{-12}$ s. (B) The field dependence of R_{1p} for three different values of the zero field splitting parameter, Δ, assuming a constant correlation time $\tau_v = 1.7 \times 10^{-13}$ s; continuous curve, $\Delta = 0.5\,cm^{-1}$; dashed curve, $\Delta = 0.9\,cm^{-1}$; and dotted curve, $\Delta = 1.3\,cm^{-1}$.

correlation time, τ_v, and the zero field splitting, Δ. This clearly suggests that the field dependence of R_{1p} can provide information about τ_v and Δ.

Therefore, the R_{1p} rates of the amide protons in HHP-Trx were measured at four different magnetic field strengths, 9.39, 11.74, 14.09, and 18.79 T. The paramagnetic relaxation enhancements were obtained from Eq. (1) using samples of 1.0 mM HHP-Trx containing equivalent amounts of Ni^{2+} and Zn^{2+}, respectively. A total of 20 amide protons with well-resolved NMR signals were included in the least squares analysis of the field dependence of the R_{1p} rates. Fig. 4 shows the field dependence of the paramagnetic relaxation enhancements for three representative amide protons. The solid curves correspond to the least squares fit of the

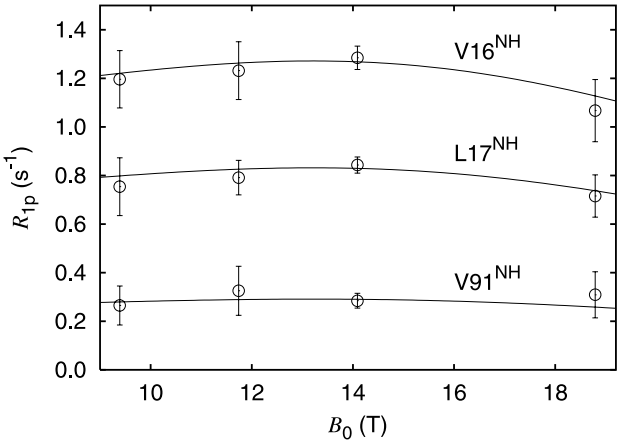

Fig. 4. The field dependence of the paramagnetic relaxation enhancement for three selected nuclei, V16^{NH}, L17^{NH}, and V91^{NH}. The curves correspond to the least squares fit of Eqs. (2)–(6).

Eqs. (2)–(6). Although the field dependence of the relaxation enhancements is only minor, the experimental data is sufficiently versatile to determine all the involved electron relaxation parameters. Thus, the parameters τ_v, Δ, and a distance r for each nucleus included in the calculation, were derived from the experimental data. Table 1 shows the parameters obtained in the fit together with the calculated electron relaxation rates at 11.74 and 18.79 T. The obtained zero field splitting, $\Delta = 1.33 \pm 0.07$ cm^{-1}, is in good agreement with the value of 1.07 ± 0.04 cm^{-1} found previously for the Ni(His)$_2^{2+}$ complex in water solution [30,31]. Moreover, $\omega_S^2\tau_v^2 = 0.12$ at 11.74 T, while $\omega_S^2\tau_v^2 = 0.32$ at 18.79 T. Accordingly, the electron relaxation rates are field dependent in the observed field range although only to a minor degree, while R_{1e} and R_{2e} are only slightly different. The R_{1e} values of $(7.6 \pm 0.9)\times10^9$ s^{-1} and $(5.4 \pm 0.6)\times10^9$ s^{-1} at 11.74 and 18.79 T, respectively, should be compared with the value of $(7.0 \pm 0.3)\times10^9$ s^{-1} obtained by method A. The fact that a reasonable value is obtained by the latter method can be ascribed to the relatively weak field dependence of R_{1e}.

The analysis here assumes that the electron relaxation mechanism is known. However, it is applicable also for mechanisms different from the zero field splitting modulation, e.g., a modulation of the anisotropy of the g-tensor [32]. In that case Eqs. (5) and (6) must be substituted by other similar equations that model the specific mechanism. Only if more than one mechanism contribute to the electron relaxation, will the method fail because of the large number of parameters involved in the analysis.

4.4. Method D: determination of R_{1e} from structure calculations using distances from the proton R_{1p} rates as constraints

The electron relaxation rate can also be determined as a parameter in a conventional structure calculation, where distances derived from R_{1p} rates are included as constraints [7]. This method requires only one magnetic field strength.

According to Eqs. (2)–(4), the electron–nucleus distances derived from the experimental R_{1p} rates depend on the electron relaxation rates. By including these distances as constraints in the calculation of the protein structure, also the energy, E_{PARA}, associated with the paramagnetic distance constraints will depend on the electron relaxation rates. Consequently, if $R_{1e} = R_{2e}$, that is if the fast-motion condition ($\omega_S^2\tau^2 \ll 1$) applies, or if the ω_S-dependent term in Eq. (2) is negligible, the electron relaxation rate, R_{1e}, can be estimated from the minimum of the E_{PARA} energy obtained in a series of structure calculations, where the size of the correlation time, $\tau_{c,1}$, is varied [7].

To obtain accurate values of the distance constraints, a Ni^{2+} titration of a 1.0 mM sample of HHP-Trx was performed, using 10 Ni^{2+} concentrations in the range from 0.0 to 2.0 mM. Thus, the variation of the longitudinal relaxation rates of the amide protons with increasing Ni^{2+} concentration was measured at 11.74 T, and the R_{1p} rates were obtained from the slope of the variations according to Eq. (7). Previously, it was found that each Ni^{2+} ion binds two protein molecules in an asymmetric dimer [8]. Also it was found that the side chain carboxylate groups of the aspartic and glutamic acid residues are weak binding sites for the Ni^{2+} ion as compared to the HHP-tag. This results in additional paramagnetic relaxation of the amide protons spatially close to these sites. However, numerous amide protons are still affected only by the HHP-bound Ni^{2+}.

Here, the structure of the asymmetric dimer complex of HHP-Trx was refined using 26 paramagnetic distance

Table 1
The electron relaxation parameters, Δ and τ_v[a,b], and the values of the longitudinal and the transverse electron relaxation rates

Δ (cm^{-1})	$\tau_v \times 10^{13}$ (s)	R_{1e}[c] $\times 10^{-9}$ (s^{-1})	R_{2e}[c] $\times 10^{-9}$ (s^{-1})	R_{1e}[d] $\times 10^{-9}$ (s^{-1})	R_{2e}[d] $\times 10^{-9}$ (s^{-1})
1.33 ± 0.07	1.70 ± 0.25	7.6 ± 0.9	9.4 ± 1.5	5.4 ± 0.6	8.2 ± 1.2

[a] Obtained in the least squares fit of the field dependence of the R_{1p} rates (method C, see text).
[b] At 298 K and pH 7.0.
[c] At a magnetic field strength of 11.74 T.
[d] At a magnetic field strength of 18.79 T.

constraints from amide protons that are affected only by the HHP-bound Ni^{2+}. The constraints were derived from the R_{1p} rates using Eq. (2). All structure calculations were carried out using the program XPLOR [33], as described previously [8]. The paramagnetic distance constraints were included in the structural refinement using the NOE square well energy function. The structure of the monomer was determined from published NOE and dihedral angle constraints [34] and fixed during the dimer refinement with the paramagnetic constraints. Initially, a value of $\tau_{c,1}$ was selected. An estimated uncertainty of 10% of the selected $\tau_{c,1}$ value and the experimental uncertainties of the R_{1p} rates were used in the calculation of the uncertainty of the paramagnetic distance constraints. Structural refinements of 60 structures were carried out and the 20 structures with the lowest *total* energy were selected. Subsequently, the 10 structures with the lowest energy of the paramagnetic distance constraints were selected for further investigation. The energy, E_{PARA}, was then calculated as the average of the energy of the paramagnetic distance constraints in these 10 structures. This procedure was repeated for a series of correlation times in the range from $\tau_{c,1} = 10^{-10.4}$ s to $\tau_{c,1} = 10^{-8.6}$ s.

Fig. 5 shows the energy of the paramagnetic distance constraints, E_{PARA}, as a function of $\tau_{c,1}$. Two local energy minima are obtained, located symmetrically around a $\tau_{c,1}$ value of $10^{-9.5}$ s. The two minima are obtained since each R_{1p} rate and thus each paramagnetic constraint corresponds to two correlation times, according to Eq. (2) and Fig. 2.

For the rotational correlation time $\tau_r = 8.76$ ns, obtained previously for the Zn^{2+} complex of HHP-Trx [8], the minima in Fig. 5 correspond to the longitudinal electron relaxation rates:

$$R_{1e} = \begin{cases} (7.8 \pm 0.5) \times 10^9\,\mathrm{s}^{-1}, \\ (1.2 \pm 0.5) \times 10^9\,\mathrm{s}^{-1}. \end{cases} \quad (9)$$

The R_{1e} rate of $(7.8 \pm 0.5) \times 10^9\,\mathrm{s}^{-1}$ is in good agreement with the value obtained by method C. However, as in the case of method A, more than one solution are obtained. Therefore, method D provides a unique electron relaxation rate only if one of the two solutions can be excluded on the basis of alternative information. Thus, for instance, if the R_{2p} rate corresponding to one of the obtained R_{1e} values exceeds the observed line width, the solution can be excluded. However, this approach does not remove the ambiguity of the solution obtained here.

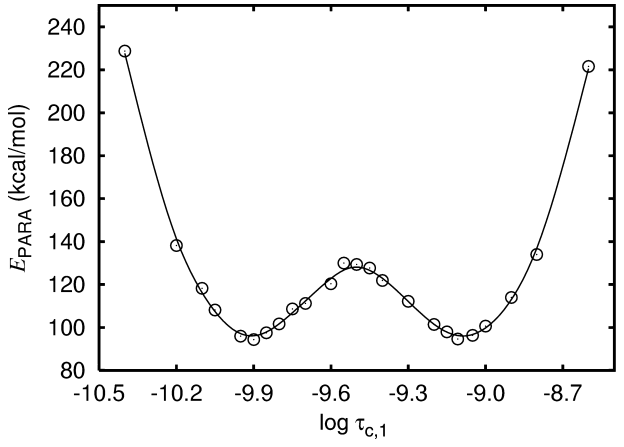

Fig. 5. The energy contribution, E_{PARA}, from the paramagnetic distance constraints to the total energy of the structure as a function of the correlation time $\tau_{c,1}$. Structural refinement of a total of 60 structures were performed for each value of the correlation time $\tau_{c,1}$. Initially, 20 structures with the lowest *total* energy were selected for further investigation. Subsequently, the energy, E_{PARA}, was calculated as the average of the energies in the 10 structures with the lowest energy of the paramagnetic distance constraints.

5. Conclusions

The study shows that the choice of NMR method for determining the electron relaxation rates, depends on whether the fast-motion condition, $\omega_S^2\tau^2 \ll 1$, applies. If the condition applies, the simpler method A can be used, that is, only the ratio of the longitudinal paramagnetic relaxation of a nucleus at two magnetic field strengths is required. If the fast-motion condition does not apply, method B can be used if, furthermore, the ω_S-dependent term in Eq. (2) is negligible. The latter condition holds for metal ions with relatively slow relaxing electrons, in particular at the high magnetic field strengths used nowadays. In that case, the R_{1e} rate can be derived from the ratios of the paramagnetic relaxation rates of two different kinds of nuclei obtained at two magnetic field strengths. On the other hand, if the ω_S-dependent term in Eq. (2) contributes significantly to the R_{1p} rate, the more elaborate method C must be used, where the paramagnetic relaxation rates of a nucleus or a number of nuclei are measured at a series of magnetic fields strengths. Unlike method A, methods B and C give unambiguous electron relaxation rates. Finally, the electron relaxation rate can be obtained from a conventional structure calculation that includes distance constraints derived from the R_{1p} rates obtained at only one magnetic field strength (method D). This method requires that the ω_S-dependent term in Eq. (2) is negligible or that the fast-motion condition applies. However, as with method A the result is ambiguous.

It should be noted, however, that irrespective of the limitations of method A and method D, it is found that both methods give rather accurate values of the electron relaxation rate of the specific Ni^{2+} protein complex investigated here, despite the fact that the electron relaxation of the unpaired electrons is somewhere between the fast-motion and the slow-motion regimes.

Acknowledgments

We thank D. Flemming Hansen and Søren M. Kristensen for helpful discussions, and Else Philipp, Jens Duus, and Bent O. Petersen for technical assistance. We are grateful to Connie Lauritzen, Søren Weis Dahl, and John Pedersen for providing the HHP-tagged thioredoxin, to Eberhard Hoffmann and Peter Sandor for recording the 400 and 600 MHz spectra, and to H. Jane Dyson for providing the NOE and torsion angle constraints of thioredoxin. The 800 MHz spectra were acquired at the Danish Instrument Center for NMR Spectroscopy of Biological Macromolecules. M.R.J. thanks Novo Nordisk A/S and Novozymes A/S for a scholarship. This work was financially supported by the Danish Natural Science Research Council (J. No.'s 9400351, 9801801, 51-00211, and 21-01-0545), Direktør Ib Henriksens Fond, Carlsbergfondet and Novo Nordisk Fonden.

References

[1] I. Bertini, C. Luchinat, G. Parigi, Solution NMR of Paramagnetic Molecules. Applications to Metallobiomolecules and Models, Elsevier, Amsterdam, 2001.
[2] J.G. Huber, J.-M. Moulis, J. Gaillard, Use of ^{1}H longitudinal relaxation times in the solution structure of paramagnetic proteins. Application to [4Fe–4S] proteins, Biochemistry 35 (1996) 12705–12711.
[3] I. Bertini, M.M.J. Couture, A. Donaire, L.D. Eltis, I.C. Felli, C. Luchinat, M. Piccioli, A. Rosato, The solution structure refinement of the paramagnetic reduced high-potential iron–sulfur protein I from *Ectothiorhodospira halophila* by using stable isotope labeling and nuclear relaxation, Eur. J. Biochem. 241 (1996) 440–452.
[4] M. Gochin, A high-resolution structure of a DNA–chromomycin-Co(II) complex determined from pseudocontact shifts in nuclear magnetic resonance, Structure 8 (2000) 441–452.
[5] M. Allegrozzi, I. Bertini, M.B.L. Janik, Y.-M. Lee, G. Liu, C. Luchinat, Lanthanide-induced pseudocontact shifts for solution structure refinements of macromolecules in shells up to 40 Å from the metal ion, J. Am. Chem. Soc. 122 (2000) 4154–4161.
[6] V. Gaponenko, A. Dvoretsky, C. Walsby, B.M. Hoffman, P.R. Rosevear, Calculation of *z*-coordinates and orientational restraints using a metal binding tag, Biochemistry 39 (2000) 15217–15224.
[7] L.W. Donaldson, N.R. Skrynnikov, W.-Y. Choy, D.R. Muhandiram, B. Sarkar, J.D. Forman-Kay, L.E. Kay, Structural characterization of proteins with an attached ATCUN motif by paramagnetic relaxation enhancement NMR spectroscopy, J. Am. Chem. Soc. 123 (2001) 9843–9847.
[8] M.R. Jensen, C. Lauritzen, S.W. Dahl, J. Pedersen, J.J. Led, Binding ability of a HHP-tagged protein towards Ni^{2+} studied by paramagnetic NMR relaxation: the possibility of obtaining long-range structure information, J. Biolmol. NMR, in press.
[9] M. Ubbink, M. Ejdebäck, B.G. Karlsson, D.S. Bendall, The structure of the complex of plastocyanin and cytochrome *f*, determined by paramagnetic NMR and restrained rigid-body molecular dynamics, Structure 6 (1998) 323–335.
[10] T.K. Mal, M. Ikura, L.E. Kay, The ATCUN domain as a probe of intermolecular interactions: application to calmodulin–peptide complexes, J. Am. Chem. Soc. 124 (2002) 14002–14003.
[11] D.F. Hansen, M.A.S. Hass, H.M. Christensen, J. Ulstrup, J.J. Led, Detection of short-lived transient protein–protein interactions by intermolecular nuclear paramagnetic relaxation: plastocyanin from *Anabaena variabilis*, J. Am. Chem. Soc. 125 (2003) 6858–6859.
[12] L. Ma, E. Philipp, J.J. Led, Determination of the electron self-exchange rates of blue copper proteins by super-WEFT NMR spectroscopy, J. Biomol. NMR 19 (2001) 199–208.
[13] M.R. Jensen, D.F. Hansen, J.J. Led, A general method for determining the electron self-exchange rates of blue copper proteins by longitudinal NMR relaxation, J. Am. Chem. Soc. 124 (2002) 4093–4096.
[14] D.F. Hansen, J.J. Led, Implications of using approximate Bloch–McConnell equations in NMR analyses of chemically exchanging systems: application to the electron self-exchange of plastocyanin, J. Magn. Res. 163 (2003) 215–227.
[15] I. Solomon, N. Bloembergen, Nuclear magnetic interactions in the HF molecule, J. Chem. Phys. 25 (1956) 261–266.
[16] N. Bloembergen, Proton relaxation times in paramagnetic solutions, J. Chem. Phys. 27 (1957) 572–573.
[17] N. Bloembergen, Comments on "Proton relaxation times in paramagnetic solutions", J. Chem. Phys. 27 (1957) 595–596.
[18] A.J. Vega, D. Fiat, Nuclear relaxation processes of paramagnetic complexes. The slow-motion case, Mol. Phys. 31 (1976) 347–355.
[19] M. Gueron, Nuclear relaxation in macromolecules by paramagnetic ions: a novel mechanism, J. Magn. Res. 19 (1975) 58–66.
[20] I. Solomon, Relaxation processes in a system of two spins, Phys. Rev. 99 (1955) 559–565.
[21] N. Bloembergen, L.O. Morgan, Proton relaxation times in paramagnetic solutions. Effects of electron spin relaxation, J. Chem. Phys. 34 (1961) 842–850.
[22] M. Rubinstein, A. Baram, Z. Luz, Electronic and nuclear relaxation in solutions of transition metal ions with spin $S = 3/2$ and 5/2, Mol. Phys. 20 (1971) 67–80.
[23] Z. Luz, S. Meiboom, Proton relaxation in dilute solutions of cobalt(II) and nickel(II) ions in methanol and the rate of methanol exchange in the solvation sphere, J. Chem. Phys. 40 (1964) 2686–2692.
[24] D.S. Wishart, B.D. Sykes, Chemical shifts as a tool for structure determination, Methods Enzymol. 239 (1994) 363–392.
[25] L. Ma, A.-M.M. Jørgensen, G.O. Sørensen, J. Ulstrup, J.J. Led, Elucidation of the paramagnetic R_1 relaxation of heteronuclei and protons in Cu(II) plastocyanin from *Anabaena variabilis*, J. Am. Chem. Soc. 122 (2000) 9473–9485.
[26] N.A. Farrow, R. Muhandiram, A.U. Singer, S.M. Pascal, C.M. Kay, G. Gish, S.E. Shoelson, T. Pawson, J.D. Forman-Kay, L.E. Kay, Backbone dynamics of a free and a phosphopeptide-complexed Src homology 2 domain studied by ^{15}N NMR relaxation, Biochemistry 33 (1994) 5984–6003.
[27] V. Gaponenko, J.W. Howarth, L. Columbus, G. Gasmi-Seabrook, J. Yuan, W.L. Hubbell, P.R. Rosevear, Protein global fold determination using site-directed spin and isotope labeling, Protein Sci. 9 (2000) 302–309.
[28] L. Ma, J.J. Led, Determination by high field NMR spectroscopy of the longitudinal electron relaxation rate in Cu(II) plastocyanin from *Anabaena variabilis*, J. Am. Chem. Soc. 122 (2000) 7823–7824.
[29] A. Carrington, G.R. Luckhurst, Electron spin resonance line widths of transition metal ions in solution. Relaxation through zero-field splitting, Mol. Phys. 8 (1964) 125–132.
[30] J.J. Led, Field dependent carbon-13 relaxation in paramagnetic nickel(II) complexes of histidine. A study of the applicability of the Solomon–Bloembergen–Morgan theories, Mol. Phys. 40 (1980) 1293–1313.

[31] J.J. Led, D.M. Grant, Carbon-13 relaxation in paramagnetic complexes of amino acids. Structural and dynamical information on nickel(II) complexes of histidine, J. Am. Chem. Soc. 99 (1977) 5845–5858.

[32] H.M. McConnell, Effect of anisotropic hyperfine interactions on paramagnetic relaxation in liquids, J. Chem. Phys. 25 (1956) 709–711.

[33] A.T. Brünger, XPLOR—A System for X-Ray Crystallography and NMR, Version 3.1, Yale University Press, New Haven, 1992.

[34] M.-F. Jeng, A.P. Campbell, T. Begley, A. Holmgren, D.A. Case, P.E. Wright, H.J. Dyson, High-resolution solution structures of oxidized and reduced *Escherichia coli* thioredoxin, Structure 2 (1994) 853–868.